Long non-coding RNA RP11-400N13.3 promotes the progression of colorectal cancer by regulating the miR-4722-3p/P2RY8 axis

HONGJU YANG[1*], QIAN LI[2*], YANRUI WU[3], JIANLONG DONG[1], YALING LAO[1], ZHENG DING[1], CHANGYAN XIAO[1], JINXIAO FU[4] and SONG BAI[1]

[1]Department of Geriatric Gastroenterology, The First Affiliated Hospital of Kunming Medical University, Kunming, Yunnan 650032; [2]Transfusion Medicine Research Department, Yunnan Kunming Blood Center, Kunming, Yunnan 650106; [3]Cell Biology and Genetics Department, Kunming Medical University, Kunming, Yunnan 650500; [4]Department of Geriatrics, The Second People's Hospital of Yunnan, Kunming, Yunnan 650201, P.R. China

Received February 15, 2020; Accepted June 29, 2020

DOI: 10.3892/or.2020.7755

Abstract. Accumulating evidence has shown that long non-coding RNAs (lncRNAs) play significant roles in the development and progression of many types of cancer including colorectal cancer. RP11-400N13.3 is a novel lncRNA discovered recently and its biological function and underlying mechanism in colorectal cancer remain elusive. This study aimed to reveal the relationship between RP11-400N13.3 and colorectal cancer. Our results demonstrated that the expression of RP11-400N13.3 was significantly upregulated in both colorectal cancer tissues and cell lines as compared to normal adjacent tissues and normal colonic epithelial cells by RT-qPCR, respectively. Upregulation of RP11-400N13.3 was found to be correlated with a poor overall survival rate. Functional studies revealed that RP11-400N13.3 facilitated the proliferation, migration, invasion and tumor growth of colorectal cancer cells while inhibiting the apoptosis of cancer cells *in vitro* and *in vivo*. We also observed that RP11-400N13.3 serves as a sponge for miR-4722-3p, and that P2Y receptor family member 8 (P2RY8) was predicted to be a target of miR-4722-3p by bioinformatics analysis. Western blot assay indicated that the expression of P2RY8 was negatively or positively regulated by miR-4722-3p or RP11-400N13.3. In addition, rescue experiments revealed that RP11-400N13.3 promoted proliferation, migration and invasion by directly regulating the expression of miR-4722-3p and P2RY8. In conclusion, our results revealed that RP11-400N13.3 promoted colorectal cancer progression via modulating the miR-4722-3p/P2RY8 axis, thus suggesting RP11-400N13.3 as a potential therapeutic target for the treatment of colorectal cancer.

Correspondence to: Dr Hongju Yang or Dr Song Bai, Geriatric Gastroenterology, The First Affiliated Hospital of Kunming Medical University, 295 Xichang Road, Wuhua, Kunming, Yunnan 650032, P.R. China
E-mail: hongjuyang105@163.com
E-mail: baisong523@163.com

*Contributed equally

Key words: RP11-400N13.3, colorectal cancer, miR-4722-3p, P2RY8

Introduction

Colorectal cancer (CRC), the third most common malignancy, is the fourth leading cause of cancer-related deaths in the world due to late tumor detection and rapid progression as CRC easily develops into a metastatic stage of growth (1,2). Approximately 90% of CRC patients can be cured by surgery at the early stage of tumor progression. Unfortunately, many CRC patients are usually diagnosed at advanced stages as a consequence of the lack of prognostic biomarkers (3). Although there are obvious improvements in the treatment strategies for CRC such as surgery, radiotherapy, chemotherapy and immunotherapy (4,5), advanced-stage patients still exhibit a poor prognosis. Moreover, the 5-year survival rate is reportedly around 40%, in different regions such as in the UK where it is 41.5% (6,7). Therefore, more research concerning CRC initiation and development is urgently required.

Long non-coding RNAs (lncRNAs) are a class of RNA molecules longer than 200 nucleotides in length without a protein-coding function. Increasing evidence suggest that the dysregulation of lncRNA expression is implicated in multiple types of cancer (8). Several studies also suggest that lncRNAs are involved in cancer-related cellular processes such as proliferation, apoptosis, migration and invasion through regulation of gene expression (9-11). In addition, lncRNAs can also serve as diagnostic or prognostic markers of various types of cancers, for instance, in hepatocellular carcinoma and prostate cancer (12-14). Various studies have reported that RP11-400N13.3 expression may serve as a prognostic biomarker for various cancers including gastric cancer, colorectal cancer, lung adenocarcinoma and breast cancer (15-19). However, the biological functions and underlying mechanisms of RP11-400N13.3 in CRC progression has yet to be elucidated.

In the present study, we first discovered that N13.3 (abbreviation of RP11-400N13.3 used in this study) serves as an oncogenic lncRNA in CRC. High expression of N13.3 was observed in both CRC patients and CRC cell lines, and was associated with poor patient prognosis. Through a series

of function-related experiments, we observed that high N13.3 expression promoted CRC cell proliferation, migration and invasion, and inhibited apoptosis by regulating the miR-4722-3p/P2Y receptor family member 8 (P2RY8) axis *in vivo* and *in vitro*. We also found that the knockdown of N13.3 reversed these experimental results successfully. In general, our results may contribute to the diagnosis and treatment of CRC.

Materials and methods

Cancer tissue samples. CRC tissues along with the adjacent non-cancerous tissues were obtained from 60 CRC patients (age: 58±9.4 years old who underwent surgery at the First Affiliated Hospital of Kunming Medical University between June 2015 and August 2019. All patients had not received any treatment and had no comorbidities. The detailed characteristics of the patients are shown in Table I. Specimens were collected and stored at -80˚C. This study was approved by the Ethics Committee of the First Affiliated Hospital of Kunming Medical University, and conducted following the Helsinki Declaration. All patients had signed a written informed consent.

Cell culture and transfection. CRC cell lines (HT-29, HCT-116, HCT-8, LoVo and RKO) as well as the normal colonic epithelial cell line (NCM460) and 293T cells were purchased from American Type Culture Collection (ATCC, USA). We authenticated the cell lines used in this study by STR profiling. The cells were cultured in Dulbecco's modified Eagle's medium (DMEM; Gibco; Thermo Fisher Scientific, Inc.) supplemented with 10% fetal bovine serum (FBS) at 37˚C, and humidified with 5% CO_2 atmosphere.

The N13.3 overexpression vector pcN13.3 and pcDNA3 (negative control), short hairpin N13.3 (sh-N13.3-1 and sh-N13.3-2) and its negative control were purchased from GenePharma. The mimics and ASO of miR-4722-3p (miR-4722-3p mimics and miR-4722-3p ASO) and the respective negative control (mimics NC and ASO NC) were purchased from RiboBio. The transfection was performed with Lipofectamine 2000 (Invitrogen; Thermo Fisher Scientific, Inc.) following the method described by the manufacturer.

Quantitative real-time PCR (RT-qPCR). The total RNA of tissues and cell lines were extracted with Trizol Reagent (Invitrogen; Thermo Fisher Scientific, Inc.) following the method described by the manufacturer. The total RNA was then reversely transcribed into complementary DNA (cDNA) using RT-PCR kit obtained from Promega Corp. Real-Time qPCR kit purchased from Qiagen was used to estimate the expression of N13.3, miR-4722-3p and P2RY8 through the instrumentation of an ABI 7500 real-time PCR system (Applied Biosystems; Thermo Fisher Scientific, Inc.). Thermocycling conditions consisted of 95˚C for 5 min, 40 cycles of 95˚C for 5 sec and 60˚C for 20 sec, 95˚C for 15 min. The primer sequences used in the study are as follows: lncRNA RP11-400N13.3-forward, 5'-TCACAGTAAGCTGCCTTCTAAGGAG-3' and lncRNA RP11-400N13.3-reverse, 5'-TGGTAAGATCCCTCGGAC TAAAACA-3'; miR-4722-3p-forward, 5'-TGCGGTGGCTGG ACGTCCCTCCA-3' and miR-4722-3p-reverse, 5'-CCAGTG CAGGGTCCGAGGT-3'; U6-forward, 5'-TGCGGGTGCTCG CTTCGGCAGC-3' and U6-reverse, 5'-CCAGTGCAGGGT CCGAGGT-3'; P2RY8-forward, 5'-CGCACCGATCTCACC TACC-3' and P2RY8-reverse, 5'-GATGGTGGCCGTGTA ACAAG-3'; GAPDH-forward, 5'-CTTCTACAATGAGCT GCGTG-3' and GAPDH-reverse, 5'-TCATGATTGAGTCAG TCAGG-3'. U6 or GAPDH was used as an endogenous control. The relative levels of expression were calculated by the $2^{-\Delta\Delta Cq}$ method (20).

Colony formation assay. CRC cells were collected after the different treatments and were seeded into a 6-well plate having a density of 1,000 cells per well, and were cultured for 2 weeks ensuring the replacement of the culture medium at 3-day intervals. Colonies were fixed with 10% formaldehyde and stained with 0.4% crystal violet in 20% ethanol for 5 min. Colonies were photographed and counted using a inverted microscope with x4 magnification (Olympus Corp.).

Cell proliferation assay. Cell proliferation assay was performed with the Cell Counting Kit-8 (CCK-8) Dojindo) following the method described by the manufacturer. In brief, transfected cells were seeded into a 96-well plate at a density of $1x10^5$ cells per well for specific time intervals (0, 24, 48 and 72 h) following the method described by the manufacturer. Absorbance was measured at 450 nm using a microliter plate reader, and in turn, the cell viability was calculated.

Transwell assay. The cell migration and invasion capacities were ascertained by Transwell assays in Transwell chamber plates (24-well plate, 8-mm pores; BD Biosciences). For invasion assay, the Transwell chamber was pre-coated with 50 μl of Matrigel (1:7 dilution; BD Bioscience) before the experiments. Cells ($5x10^4$ cells) following the different treatments were placed in serum-free medium and were added into the top chambers, with the lower chamber filled with DMEM containing 10% FBS. After incubation for 24 h, the chambers were fixed using 4% paraformaldehyde and stained with 0.1% crystal. Stained cells in the lower chambers were counted in three randomly selected fields with the aid of a inverted microscope with a magnification, x4 (Olympus Corp.). For the migration assay, a Transwell chamber without pretreatment with Matrigel was used, while the other steps were the same as the invasion assay.

RNA pull-down assay. In order to determine the existence of mutual interaction between N13.3 and miR-4722-3p, RNA pull-down assay was performed with a T7 Megascript kit (Thermo Fisher Scientific, Inc.) following the method described by the manufacturer. In addition, expression of miR-4722-3p was detected by RT-qPCR.

Luciferase reporter assay. The interaction between miR-4722-3p-N13.3 and miR-4722-3p-P2RY8 was determined by dual-luciferase reporter assay. In brief, sequences of N13.3 or P2RY8 3'UTR containing wild-type or mutated sites of miR-4722-3p were synthesized. Cells were co-transfected with luciferase reporter vectors and miR-4722-3p mimic/ASO, alongside their respective negative controls using Lipofectamine 2000. After transfection for 48 h, the luciferase activity was measured by the dual-luciferase reporter assay system (Promega Corp.).

Table I. Relationship between N13.3 expression and clinicopathological features (n=60).

Characteristics	n	N13.3 expression		P-value
		Low (n=30)	High (n=30)	
Age, years				0.605
<60	32	15	17	
≥60	28	15	13	
Sex				0.795
Female	33	16	17	
Male	27	14	13	
Tumor size, cm				0.001[a]
≤5	36	25	11	
>5	24	5	19	
Tumor location				0.793
Rectum	35	17	18	
Colon	25	13	12	
TNM stage				0.004[a]
I/II	27	19	8	
III/IV	33	11	22	
Lymph node metastasis				0.028[a]
No	42	24	16	
Yes	20	6	14	
Distant metastasis				0.023[a]
No	54	29	23	
Yes	8	1	7	

Low or high expression of N13.3 as determined by the sample median. [a]P<0.05 was considered statistically significant (χ^2 test). TNM, Tumor Node Metastasis.

Western blot analysis. Total protein was extracted from cells or tissues with RIPA buffer (Sigma-Aldrich; Merck KGaA). Protein concentration was determined by the Bicinchoninic Acid (BCA) protein assay (Beyotime Biotechnology). The 30 μg protein extracts were separated by 10% SDS-PAGE, and then transferred onto polyvinylidene difluoride (PVDF) membranes. The membranes were blocked by dipping them in 5% non-fat milk at room temperature for 1 h, and incubated with primary antibodies against caspase-3 [product no. 9662S, Cell Signaling Technology, Inc. (CST)], Bcl2, (ab32124; Abcam), Bax (product no. 5023S; CST), P2RY8 (cat. no. ABP52106; Abbkine) and GAPDH (product no. 51332S; CST) overnight. All primary antibodies were diluted with 5% non-fat milk dissolved in 1X TBST. Furthermore, the membranes were incubated with secondary antibodies anti-rabbit (product no. 7074S; CST) and anti-mouse (product no. 7076S; CST) at room temperature for 1 h; the secondary antibody was combined with horseradish peroxidase. All secondary antibodies were also diluted with 5% non-fat milk dissolved in 1X TBST. The generated signal for the protein-antibody complex was detected by enhanced chemiluminescence (ECL) substrate (Millipore). Protein quantification was completed with ImageJ 1.8.0 (National Institute of Mental Health).

Tumor xenograft assay. All animal experiments were approved by the Ethics Committee of the First Affiliated Hospital of Kunming Medical University. A total of 48 males BALB/c nude mice (age: 4-weeks; weight: 17-23 g) were obtained from Beijing HFK Bioscience. Mice were housed in an SPF environment with 40-60% relative humidity at 22-24˚C with a 12-h light/dark cycle and free access to water and food. The mice were randomly divided into two groups (six per group), and then injected subcutaneously with $5x10^6$ HT-29 cells in 200 μl PBS transfected with sh-NC/sh-N13.3, pcDNA3/pcN13.3, mimics NC/miR-4722-3p mimics and ASO NC/miR-4722-3p ASO, respectively. Tumor size was measured at an interval of 4 days, and tumor volume (V) was calculated as V=length x width^2/2. After 24 days, the nude mice were sacrificed and tumors were excised for further investigation.

Lung metastasis model. HT-29 cells ($1x10^6$) infected with sh-NC or sh-N13.3 were injected into the tail vein of the nude mice (n=6). After 7 weeks, mice were sacrificed and lung metastasis was assessed by counting the number of tumor nodules, and the weight of the lung was subsequently weighed. In addition, H&E staining was used to evaluate lung metastasis.

Apoptosis assay. Cells were transfected for 48 h and collected in binding buffer. Cells were stained with Annexin V-FITC for 10 min, and PI for 5 min (Beyotime Institute of Biotechnology), following the method described by the manufacturer. The rate of apoptosis in cells was estimated by flow cytometry (FACScan; BD Biosciences).

Bioinformatics analysis. Multiple lncRNA expression in CRC patients and normal individuals was analyzed with NONCODE database (http://www.noncode.org/index.php). Refseq database (https://www.ncbi.nlm.nih.gov/refseq/) was also used to analyzed the expression of lncRNAs in CRC patients. RegRNA 2.0 database was used to predict the target of N13.3 (http://regrna2.mbc.nctu.edu.tw/). P2RY8 was found to be a potential target of miR-4722-3p by Targetscan online software (http://www.targetscan.org/vert_71/).

Statistical analysis. Data are expressed as the mean ± standard deviation (SD) of at least three separate experiments, and analyzed using GraphPad Prism 5 software (GraphPad Software, Inc.) and SPSS 20 software (IBM, Corp.). Differences between the two groups were assessed with Student's independent t-test. The relationship between N13.3, P2RY8 and miR-4722-3p was determined by Spearman's correlation. Chi-square test was employed to assess the clinical relationship between N13.3 expression and tumor features. One way ANOVA was used to analyze data from multiple groups. The overall survival curve was analyzed using the Kaplan-Meier method and log-rank test. The expression of N13.3, miR-4722-3p, and P2RY8 was analyzed by paired t-test in cancer tissues of CRC patients. P<0.05 was considered to indicate a statistically significant difference.

Results

N13.3 is highly expressed in CRC tissues and cell lines. We firstly analyzed the level of expression of multiple lncRNAs in CRC patients and normal individuals with NONCODE

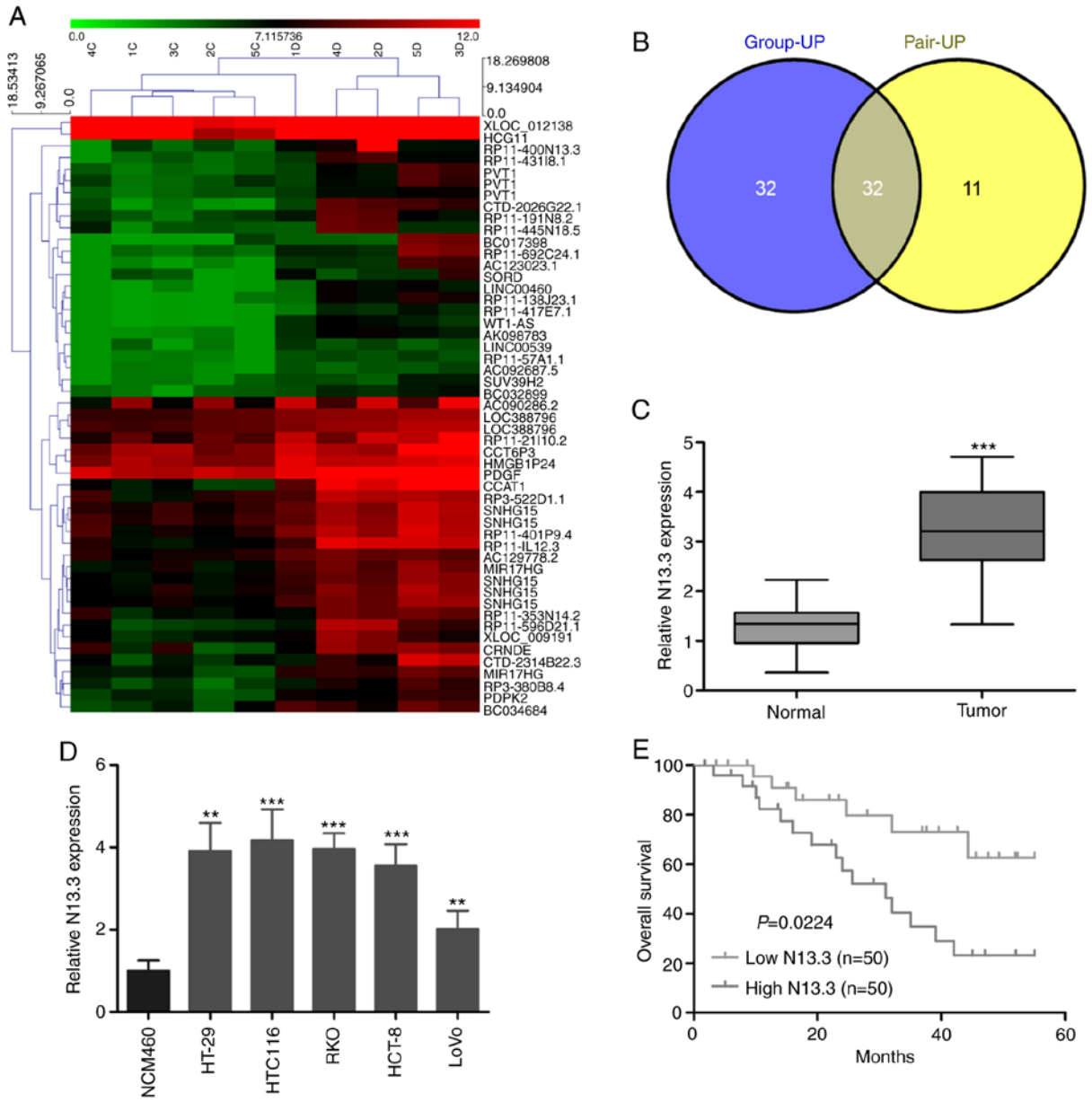

Figure 1. N13.3 is highly upregulated in CRC tissues and cells. (A) Heatmap of lncRNA expression in human CRC tissues and adjacent noncancer tissues. (B) The 32 common upregulated lncRNAs were analyzed by NONCODE and Refseq database. (C) Expression levels of N13.3 were detected in CRC tumor and adjacent noncancer tissues using RT-qPCR (n=60). ***P<0.001, compared to the normal tissues. (D) Expression levels of N13.3 were determined in CRC cell lines (HT-29, HCT-116, HCT-8, LoVo and RKO) and normal colonic epithelial cell line (NCM460) by RT-qPCR. **P<0.01 and ***P<0.001, compared to the NCM460 cells. (E) Kaplan-Meier analysis was used to analyze the correlation between N13.3 expression levels and overall survival in patients with CRC. The median N13.3 expression of all patients was used as the cut-off value to separate high vs. low group. Data are expressed as the Means ± SD. Statistical analysis was conducted using paired t-test and Kaplan-Meier analysis. **P<0.01 and ***P<0.001. N13.3, RP11-400N13.3; CRC, colorectal cancer; lncRNA, long non-coding RNA.

database (http://www.noncode.org/index.php). The relationship between N13.3 expression and clinical features of the CRC patients is shown in Table I. The heatmap indicated that N13.3 was highly expressed in CRC patients compared with normal individuals (Fig. 1A). Further investigation revealed that 32 lncRNAs were overexpressed in CRC in NONCODE and Refseq database (https://www.ncbi.nlm.nih.gov/refseq/) (Fig. 1B). In addition, the expression of N13.3 in CRC 60 cancer tissues and corresponding adjacent normal tissues was detected by RT-qPCR. We found that the expression of N13.3 was upregulated in CRC tissues when compared with that in corresponding adjacent normal tissues (Fig. 1C). Similarly, high expression of N13.3 was found in CRC cell lines when compared with that in the normal colonic epithelial cells (Fig. 1D). We also found that the overexpression of N13.3 was correlated with poor overall survival of CRC patients (Fig. 1E). This results indicate that N13.3 may play a pivotal role in CRC.

Knockdown of N13.3 inhibits proliferation, migration and invasion, and reduces apoptosis of CRC cells. To further investigate the role of N13.3 in CRC cells, HT-29 and HCT-116 cells were transfected with sh-N13.3 or sh-NC and transfection efficiency was measured by RT-qPCR (Fig. 2A). CCK-8 assay revealed that the proliferative ability of CRC cells was significantly suppressed by the knockdown of N13.3 (Fig. 2B and C). Consistently, we observed that the rate of apoptosis in cells

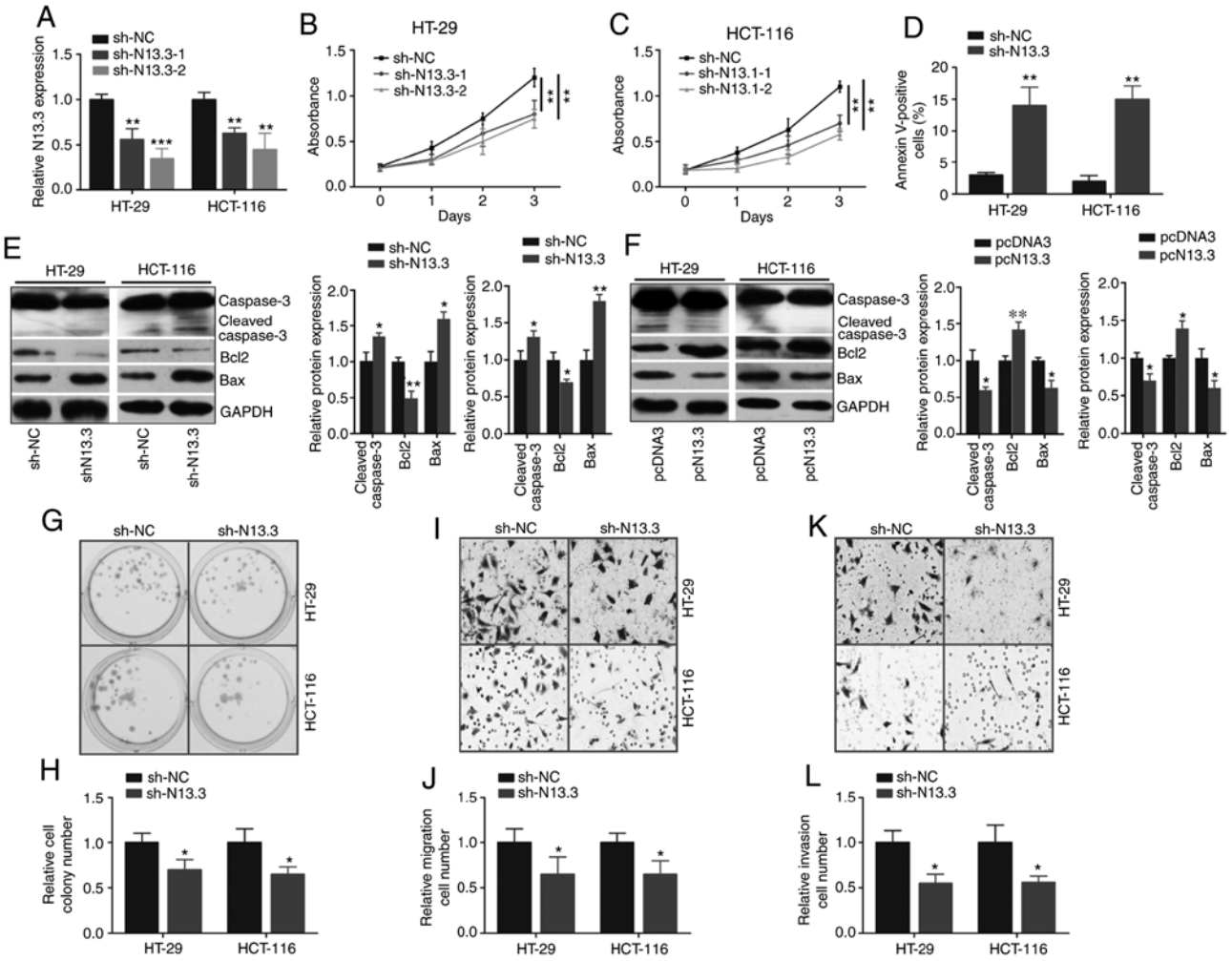

Figure 2. Knockdown of N13.3 inhibits CRC proliferation *in vitro*. HT-29 and HCT-116 cells were transfected with sh-NC or sh-N13.3. (A) Expression of N13.3 was assessed using RT-qPCR. **P<0.01 and ***P<0.001, compared with the sh-NC group. (B and C) Cell viability was examined in HT-29 and HCT-116 cells by CCK-8 assay at different time points. **P<0.01, compared to the sh-NC group. (D) Cell apoptosis rates were detected by flow cytometry. **P<0.01, compared to the sh-NC group. (E and F) Western blot analysis of the expression of apoptosis-related markers, caspase-3, Bcl2, Bax after transfection of the CRC cells with sh-N13.3 or pcN13.3. *P<0.05, **P<0.01, compared with the sh-NC or pcDNA3 group. (G and H) Colony formation assay was performed in HT-29 and HCT-116 cells following transfection with sh-N13.3. *P<0.05, compared with the sh-NC group. (I-L) Transwell assays carried out to evaluate the migration and invasion capacities of HT-29 and HCT-116 cells transfected with sh-NC or sh-N13.3. *P<0.05, compared with the sh-NC group. Data are expressed as the Means ± SD. Statistical analysis was conducted using Student's t-test and One-way ANOVA analysis. *P<0.05, **P<0.01 and ***P<0.001. N13.3, RP11-400N13.3; CRC, colorectal cancer.

was significantly elevated following the knockdown of N13.3, as compared with sh-NC group (Figs. S1A and 2D). We also analyzed the expression of apoptotic proteins. The results showed that caspase-3 and Bax were significantly increased, and Bcl2 was significantly decreased in the HT-29 and HCT-116 cells transfected with sh-N13.3 when compared with the sh-NC group (Fig. 2E). The role of N13.3 in the inhibition of cell apoptosis was confirmed by detecting the expression of caspase-3, Bax and Bcl2 in HT-29 and HCT-116 cells having highly expressed N13.3 (Fig. 2F). In addition, colony formation and Transwell invasion assays revealed that the knockdown of N13.3 greatly reduced the colony formation, migration and invasion capacity of HT-29 and HCT-116 cells (Fig. 2G-L).

To further validate the function of N13.3 in CRC cells, we upregulated the expression of N13.3 and ascertained the effect on proliferation, migration and invasion of CRC cells. We found that the expression of N13.3 was successfully increased in CRC cells transfected with pcN13.3 (Fig. 3A). As expected, the cell proliferation, colony formation, migration and invasion capacity were significantly enhanced following transfection of pcN13.3 into the CRC cells (Fig. 3B-I).

N13.3 functions as a molecular sponge for miR-4722-3p in CRC cells. In this study, the RegRNA 2.0 database (http://regrna2.mbc.nctu.edu.tw/) predicted N13.3 as a potential downstream target of miR-4722-3p (Fig. 4A). To ascertain the potential binding between miR-4722-3p and N13.3, the luciferase reporter assay was performed. In briefly, HT-29 cells were transfected with N13.3 [wild-type (wt) and mutant (mut), respectively] luciferase reporter vector and miR-4722-3p (miR-4722-3p mimics and miR-4722-3p ASO, respectively). Results showed that miR-4722-3p mimics inhibited luciferase activity (Fig. 4B). However, it was enhanced by miR-4722-3p ASO (Fig. 4C). Furthermore, we detected the expression of miR-4722-3p in CRC cell lines and tissues. The results revealed that miR-4722-3p was significantly downregulated in the CRC cell lines and cancer tissues as compared to the control groups (Fig. 4D and E). Furthermore, RNA pull

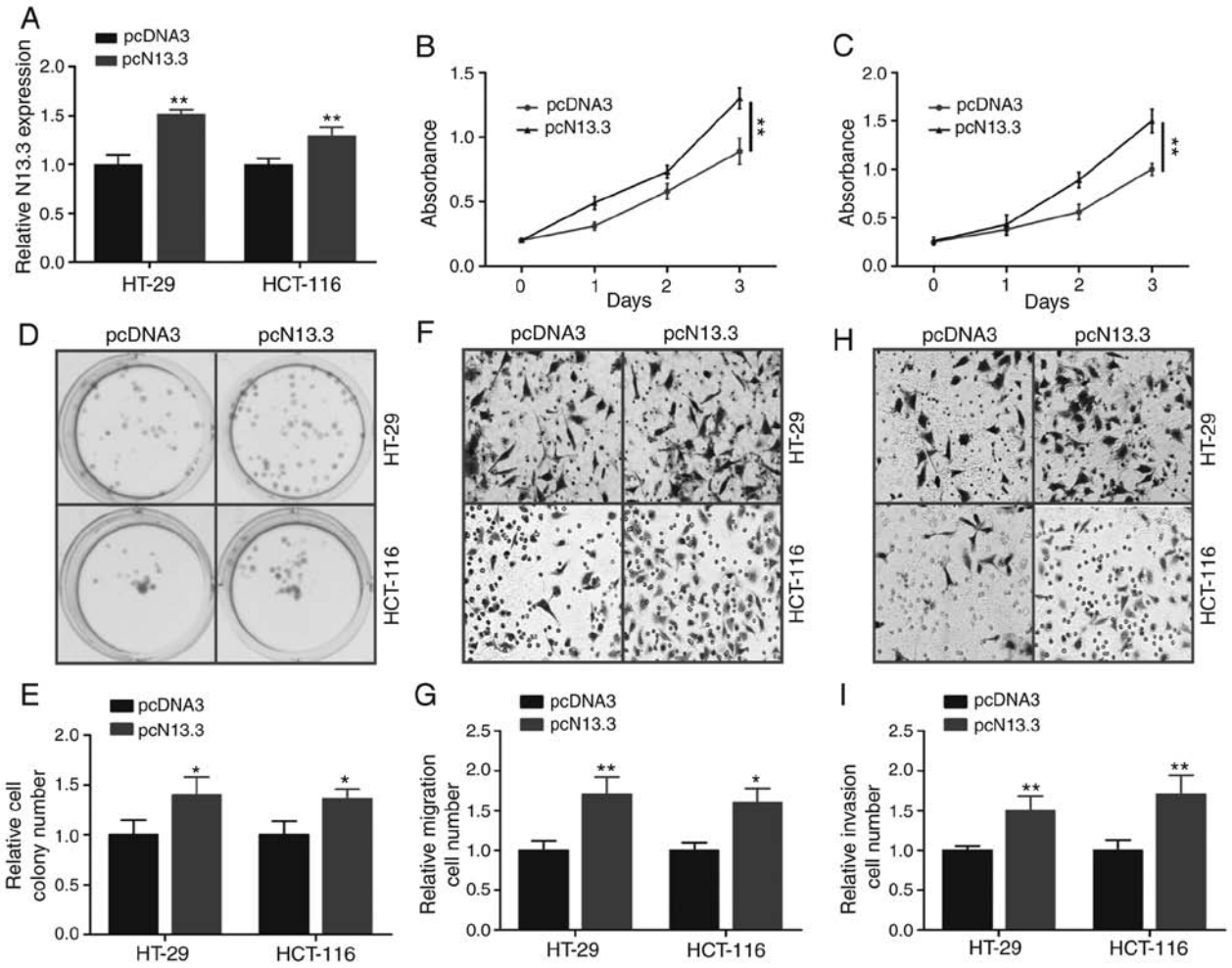

Figure 3. Overexpression of N13.3 promotes CRC proliferation *in vitro*. HT-29 and HCT-116 cells were transfected with pcDNA3 or pcN13.3. (A) Expression of N13.3 was measured using RT-qPCR. **P<0.01, compared with the pcCNA3 group. (B and C) Cell viability was examined in HT-29 and HCT-116 cells by CCK-8 assay. **P<0.01, compared with the pcCNA3 group. (D and E) Colony formation assay was performed in HT-29 and HCT-116 cells. *P<0.05, compared with the pcDNA3 group. (F-I) Transwell assays were carried out to evaluate the migration and invasion capacities of HT-29 and HCT-116 cells transfected with pcDNA3 or pcN13.3. *P<0.05 and **P<0.01, compared with the pcDNA3 group. Data are expressed as the Means ± SD. Statistical analysis was conducted using Student's t-test. *P<0.05 and **P<0.01. N13.3, RP11-400N13.3; CRC, colorectal cancer.

down assay revealed that miR-4722-3p was enriched in the N13.3 overexpression group as compared to the pcDNA3 group (Fig. 4F). To further validate these results, HT-29 and HCT-116 cells were transfected with pcN13.3/sh-N13.3 and negative control, respectively. We found that the expression of miR-4722-3p was significantly decreased in cells transfected with pcN13.3 compared to the negative control group (Fig. 4G), while sh-N13.3 induced an upregulation of miR-4722-3p (Fig. 4H). To study the effect of miR-4722-3p on CRC cells, we first confirmed the overexpression or knockdown efficiency of miR-4722-3p in CRC cells transfected with miR-4722-3p mimics or ASO (Fig. S1D and E). Next, we found that the expression of N13.3 was significantly decreased or increased in the cells transfected with miR-4722-3p mimics or ASO, respectively (Fig. 4I and J). In addition, N13.3 was negatively correlated with miR-4722-3p in the clinical samples (Fig. 4K). Finally, we observed that miR-4722-3p mimics/ASO markedly suppressed/promoted the proliferation, colony formation, migration and invasion of HT-29 and HCT-116 cells, but these results were reversed in cells transfected with pcN13.3/sh-N13.3 (Figs. 4L-O and S1B and C).

P2RY8 is a direct target of miR-4722-3p in CRC cells. We further predicted P2RY8 as a potential downstream target of miR-4722-3p by Targetscan online software (http://www.targetscan.org/vert_71/) (Fig. 5A). To determine whether miR-4722-3p effectively targets P2RY8, the luciferase reporter assay was employed. The results showed that the simulation of miR-4722-3p distinctly inhibited the luciferase activity of P2RY8-WT reporter (Fig. 5B), while miR-4722-3p ASO significantly increased luciferase activity of P2RY8-WT reporter (Fig. 5C). However, the miR-4722-3p mimics or ASO exhibited no function on the luciferase activity of cells transfected with mutated P2RY8 luciferase reporter (Fig. 5B and C). In addition, the RT-qPCR experiment revealed a significantly high level of expression of P2RY8 in the CRC cell lines and cancer tissues compared to the NCM460 cells and the normal tissue (Fig. 5D and E). In addition, miR-4722-3p mimics significantly downregulated P2RY8 expression in the HT-29 and HCT-116 cells (Fig. 5F). Correspondingly, miR-4722-3p ASO upregulated P2RY8 expression in the HT-29 and HCT-116 cells (Fig. 5G). Simultaneously, a negative and positive correlation was noted between miR-4722-3p and P2RY8, and

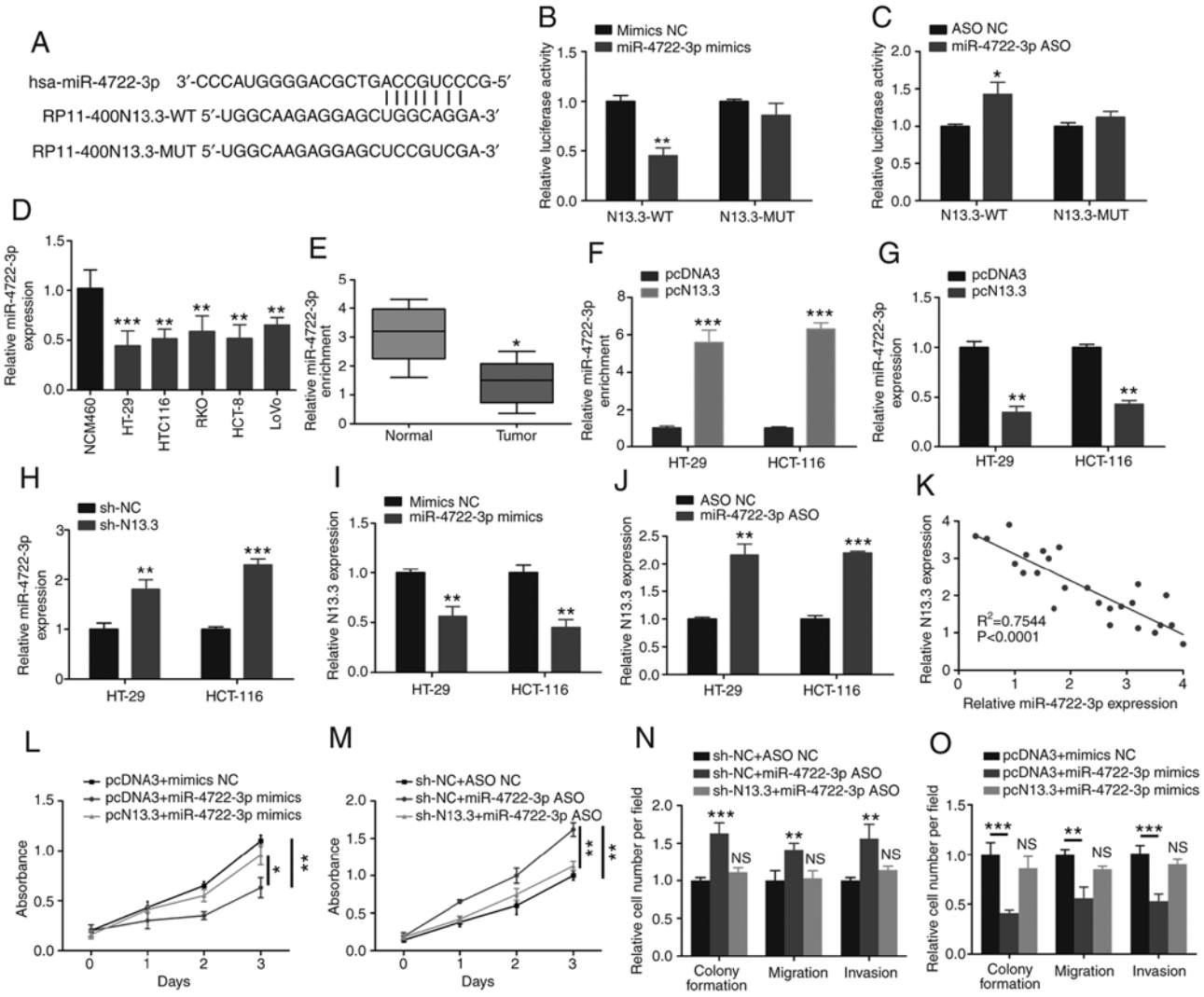

Figure 4. N13.3 functions as a molecular sponge for miR-4722-3p in CRC cells. (A) Bioinformatics software Targetscan predicted the binding sites of miR-4722-3p on N13.3, and the mutated sequence is presented. (B) Luciferase reporter assay was performed to detect the luciferase activity of reporter vector in HT-29 cells transfected with N13.3-WT/MUT and mimics NC/miR-4722-3p mimics. **P<0.01, compared with the mimics NC group. (C) Luciferase reporter assay was used to detect the luciferase activity of reporter vector in HT-29 cells transfected with N13.3-WT/MUT and ASO NC/miR-4722-3p ASO. *P<0.05, compared with the ASO NC group. (D) Expression levels of miR-4722-3p were detected in CRC cell lines and normal colonic epithelial cell line NCM460 by RT-qPCR. **P<0.01 and ***P<0.001, compared with the NCM460 cell line. (E) Expression levels of miR-4722-3p were detected in CRC tumor and normal tissues using RT-qPCR (n=60). *P<0.05, compared with the normal tissues. (F) Enrichment of miR-4722-3p was measured in HT-29 cells transfected with pcDNA3 or pcN13.3 using RNA-pull down assay. ***P<0.001, compared with the pcDNA3 group. (G and H) Expression of miR-4722-3p was determined in HT-29 and HCT-116 cells transfected with pcDNA3/pcN13.3 or sh-NC/sh-N13.3 using RT-qPCR. **P<0.01 and ***P<0.001, compared with the pcDNA3 or sh-NC group. (I and J) Expression of N13.3 in HT-29 and HCT-116 cells transfected with mimics NC/miR-4722-3p mimics or ASO NC/miR-4722-3p ASO. **P<0.01 and ***P<0.001, compared with the mimics NC or ASO NC group. (K) The correlation was analyzed between N13.3 and miR-4722-3p expression in the CRC cancer tissues. (L and M) CCK-8 assay was used to verify the role of N13.3 and miR-4722-3p in HT-29 cells proliferation. *P<0.05, **P<0.01. (N and O) Colony formation assay and Transwell assays were carried out to determine the correlation between N13.3 and miR-4722-3p in HT-29 cell colony formation, migration and invasion. NS, not significant, *P<0.05, **P<0.01 and ***P<0.001. Data are expressed as the means ± SD. Statistical analysis was conducted using Student's t-test, paired t-test and One-way ANOVA analysis. *P<0.05, **P<0.01 and ***P<0.001; NS, not significant. N13.3, RP11-400N13.3; CRC, colorectal cancer.

between N13.3 and P2RY8, respectively, in the CRC tissues (Fig. 5H and I) and this was further investigated by western blot analysis (Fig. 5J and K).

Knockdown of N13.3 inhibits CRC tumor growth in vivo. To explore the effects of N13.3 and miR-4722-3p on CRC cell tumorigenesis in animal models, HT-29 cells were transfected with sh-N13.3/pcN13.3 or miR-4722-3p mimics/ASO, and were injected subcutaneously into male nude mice. The results showed that the knockdown of N13.3 inhibited tumor growth, but the tumors formed from the N13.3-overexpressing HT-29 cells showed faster growth rates when compared to the control group (Fig. 6A and F). The tumor weight was significantly lower in the sh-N13.3 group as compared to the control group. In contrast, a significantly higher tumor weight was observed in the N13.3-overexpressing group when compared to the control group (Fig. 6B and G). The expression of N13.3 and P2RY8 was decreased in the sh-N13.3 group (Fig. C and E) while N13.3 and P2RY8 was significantly increased in the HT-29 cells transfected with pcN13.3 (Fig. 6H and J). In addition, miR-4722-3p expression was assessed in the tumor tissues of

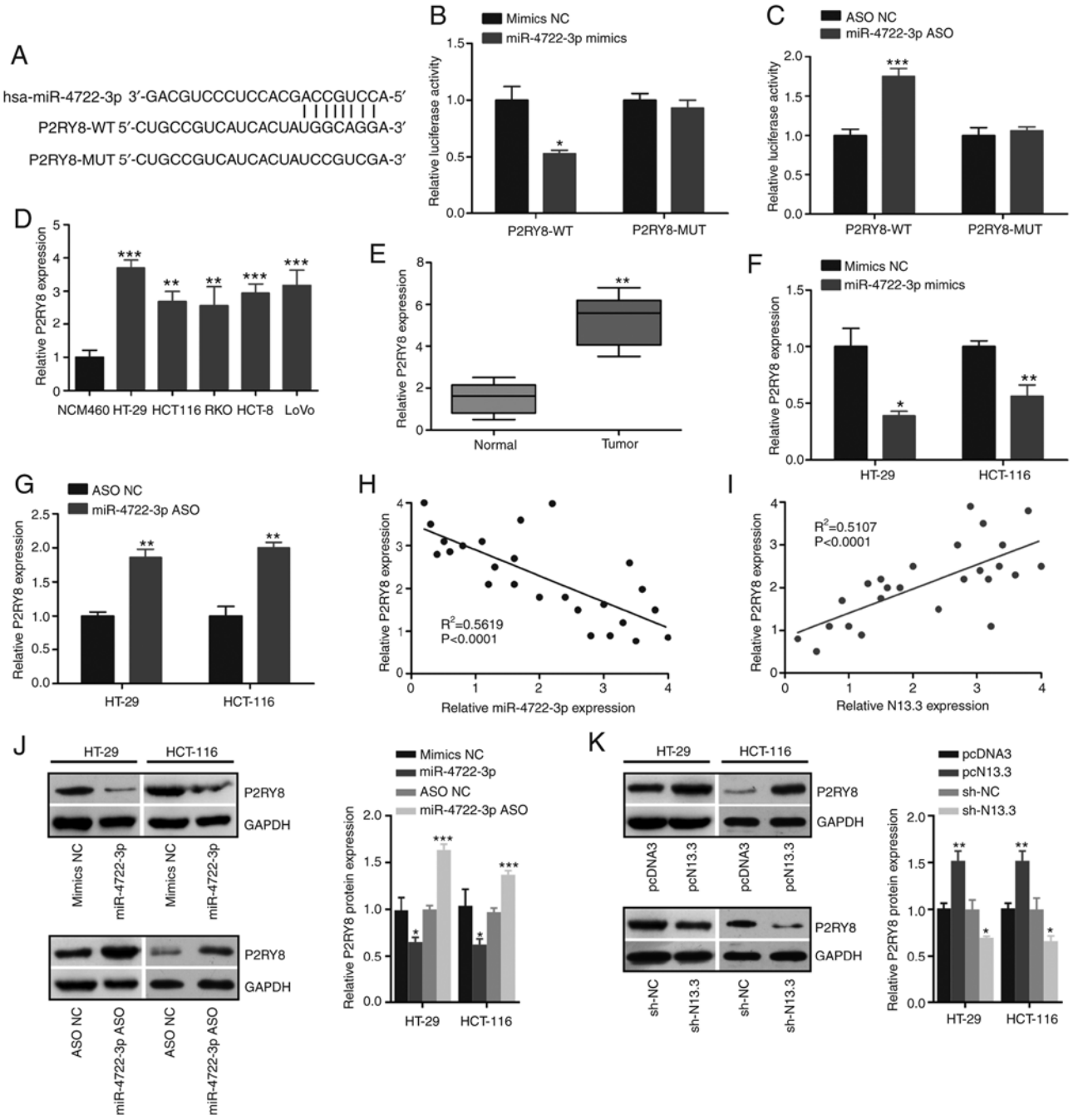

Figure 5. P2RY8 is a direct target of miR-4722-3p. (A) The binding sites between miR-4722-3p and P2RY were predicted using Targetscan. (B) Luciferase reporter assay was performed in 293T cells transfected with P2RY8-WT/MUT and mimics NC/miR-4722-3p mimics. *P<0.05, compared with the mimics NC group. (C) Luciferase activity in 293T cells transfected with P2RY8-WT/MUT and ASO NC/miR-4722-3p ASO. ***P<0.001, compared with the ASO NC group. (D) P2RY8 expression was detected in CRC cell lines and normal colonic epithelial cell line NCM460 by RT-qPCR. **P<0.01 and ***P<0.001, compared with the NCM460 cells. (E) RT-qPCR was used to analyze the expression of P2RY8 in CRC tumor and normal tissues (n=60). **P<0.01, compared with the normal tissues. (F and G) Expression of P2RY8 was measured in HT-29 and HCT-116 cells transfected with mimics NC/miR-4722-3p and ASO NC/miR-4722-3p ASO by RT-qPCR. *P<0.05, **P<0.01, compared to the mimics NC or ASO NC group. (H) The correlation was analyzed between P2RY8 and miR-4722-3p expression levels in CRC cancer tissues. (I) The correlation between P2RY8 and N13.3 expression in CRC cancer tissues. (J) The expression of P2RY8 was measured in HT-29 and HCT-116 cells transfected with mimics NC/miR-4722-3p mimics or ASO NC/miR-4722-3p ASO by western blot analysis. *P<0.05 and ***P<0.001, compared to the mimics NC or ASO NC group. (K) P2RY8 expression level in HT-29 and HCT-116 cells transfected with pcDNA3/pcN13.3 or sh-NC/sh-N13.3. *P<0.05 and **P<0.01, compared to the sh-NC or pcDNA2 group. Data are expressed as the Means ± SD. Statistical analysis was conducted using Student's t-test, paired t-test and One-way ANOVA analysis. *P<0.05, **P<0.01 and ***P<0.001. P2RY8, P2Y receptor family member 8; CRC, colorectal cancer.

the N13.3-knockout and overexpressing groups by RT-qPCR (Fig. 6D and I). In addition, we found that the tumor growth was suppressed in the miR-4722-3p mimics group and promoted in miR-4722-3p ASO group (Fig. 6K and M). Subsequently, the tumor weight was significantly lower in the miR-4722-3p mimics group and higher in the miR-4722-3p ASO groups (Fig. 6L and N). Low expression of N13.3 significantly inhibited the lung metastasis of HT-29 cells *in vivo* (Fig. 6O and P). H&E staining showed that low expression of N13.3 inhibited lung metastasis (Fig. 6Q).

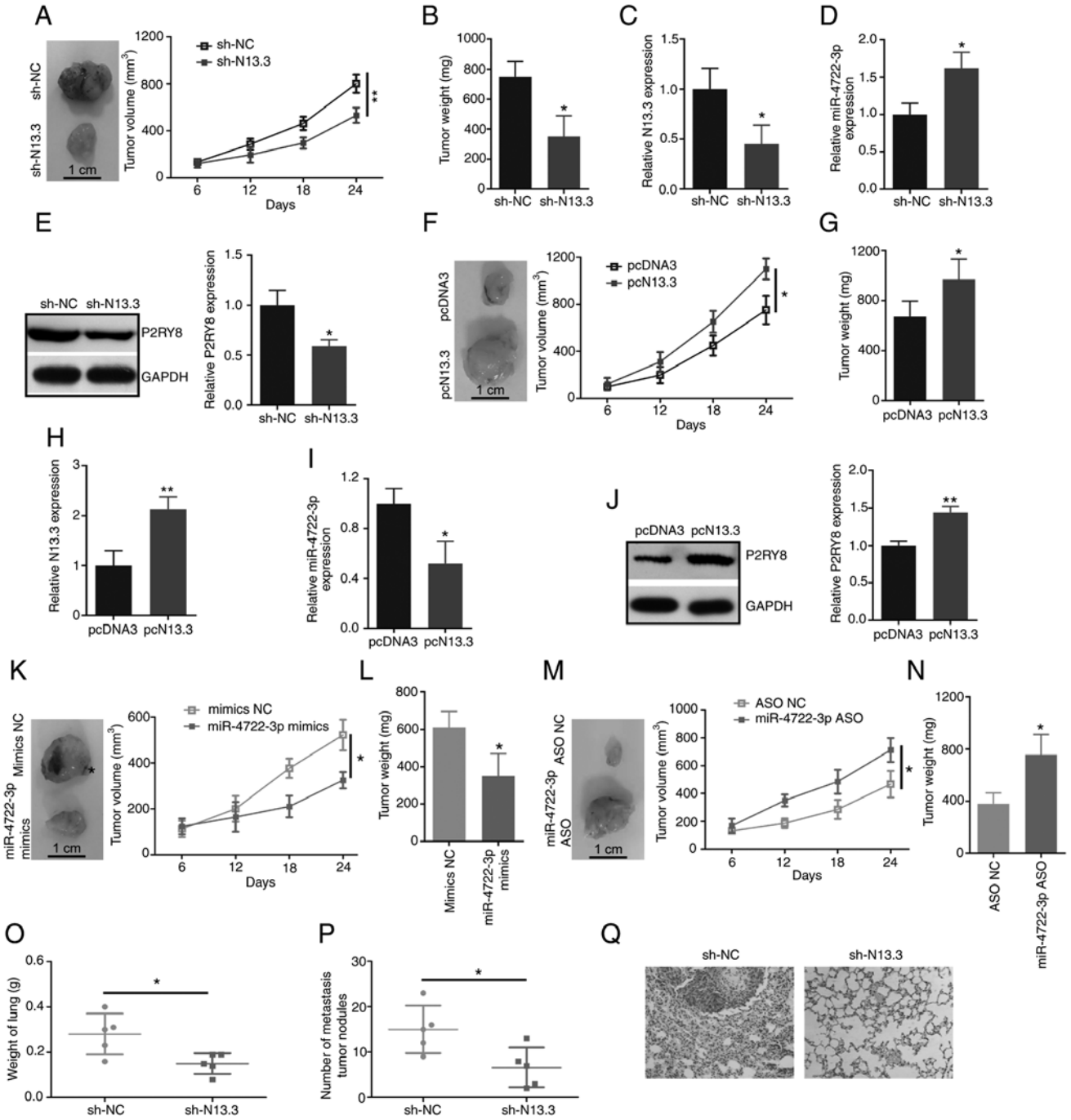

Figure 6. Knockdown of N13.3 inhibits CRC tumor growth *in vivo*. (A and F) Tumor volume was measured and growth curve was drawn in N13.3 knockdown or overexpression groups. *P<0.05 and **P<0.01, compared with the sh-NC or pcDNA3 group. (B and G) Tumour weight from both the N13.3 knockdown or overexpression groups is presented (n=6). *P<0.05, compared with the sh-NC or pcDNA3 group. (C and H) RT-qPCR was used to detect the expression of N13.3 in the N13.3 knockdown and overexpression tumor tissues. *P<0.05 and **P<0.01, compared with the sh-NC or pcDNA3 group. (D and I) Expression levels miR-4722-3p were detected by RT-qPCR in the N13.3 knockdown and overexpression tumor tissues. *P<0.05, compared with the sh-NC or pcDNA3 group. (E and J) Western blotting was used to detect P2RY8 expression in N13.3 knockdown and overexpression tumor tissues. *P<0.05 and **P<0.01, compared with the sh-NC or pcDNA3 group. (K and M) Tumor volume was measured and growth curve was drawn in miR-4722-3p mimic and miR-4722-3p ASO groups. *P<0.05, compared to the mimics NC or ASO NC group. (L and N) Tumour weight in the miR-4722-3p mimic and miR-4722-3p ASO groups. (n=6). (O) The weight of lung in the two groups. *P<0.05. (P) Number of metastasis tumor nodules in lung of nude mice injected with HT-29 cells transfected with sh-NC or sh-N13.3. *P<0.05. (Q) H&E staining of tumor lung metastasis in sh-NC and sh-N13.3 groups. Data are expressed as the Means ± SD. Statistical analysis was conducted using Student's t-test. *P<0.05 and **P<0.01. N13.3, RP11-400N13.3; CRC, colorectal cancer; P2RY8, P2Y receptor family member 8.

Discussion

Colorectal cancer (CRC) is a type of human malignant tumor. Many CRC patients succumb to the disease due to the lack of sufficient diagnostic markers and poor understanding of the pathological mechanism. Thus, there is an urgent need to elucidate the pathological mechanisms of CRC. Recently, several reports have revealed that a growing number of long non-coding RNAs (lncRNAs) play key roles in the development and progression of cancers, including CRC (11,21).

Numerous studies have also documented that the aberrant expression of lncRNAs, such as lncRNA OCC-1 (21), lncRNA HOXB-AS3 (22), CCAL (23) and lncRNA CCAT1-L (24), are involved in proliferation, poor prognosis, overall survival rate, metastasis, migration and invasion of CRC. Previous studies have also found that abnormal N13.3 expression is associated with the progression of cancer. For example, although it was found that lncRNA N13.3 expression was upregulated (and may be a prognostic marker) in gastric cancer, the biological function of N13.3 has not be extensively studied (15,17). In the present study, the function of N13.3 in CRC was revealed for the first time. We found that the level of expression of N13.3 was significantly increased in CRC cancer tissues compared with that noted in the corresponding adjacent normal tissues of CRC patients. Analogous results were found in CRC cell lines. In addition, high expression of N13.3 was directly associated with an unsatisfactory overall survival rate of CRC patients. These results indicated that the expression level of N13.3 was intimately associated with progression and prognosis of CRC patients. For the purpose of ascertaining the roles of N13.3 in CRC, a series of functional experiments were executed *in vitro* and *in vivo*. Our results demonstrated that the proliferation, cell colony formation, migration and invasion capacities were significantly inhibited while cell apoptosis was increased due to the knockdown of N13.3; however, upregulation of N13.3 expression reversed these results. Furthermore, we demonstrated that the tumor growth was successfully suppressed by the knockdown of N13.3. Thus, our findings indicate that N13.3 plays a carcinogenic function in CRC.

Meanwhile, many studies have shown that one of the roles of lncRNAs is to regulate gene expression by competitively binding to miRNAs as competing endogenous RNAs (ceRNAs) in cancers. For instance, lncRNA linc00645 and SMAD5-AS1 have been reported as ceRNAs to mediate the progression of glioma and nasopharyngeal carcinoma by targeting miR-205-3p and miRNA-106a-5p, respectively (25,26). In the present study, we predicted miR-4722-3p as a potential downstream target of N13.3 by NONCODE database analysis. The prediction result was validated by luciferase reporter assay. There are few scientific studies concerning miR-4722-3p, especially in cancers. Therefore, our study was the first to investigate the biological functions of miR-4722-3p. We demonstrated that the level of expression of miR-4722-3p was inversely regulated by N13.3 both in CRC cell lines and cancer tissues. This result was validated by overexpressing or underexpressing one variable and then detecting the level of expression of the other variable using RT-qPCR. Simultaneously, elevated expression of miR-4722-3p significantly inhibited CRC cell proliferation, colony formation, migration and invasion ability, which were all reversed by overexpression of N13.3. Expectedly, this negative regulation was found in HT-29 cells transfected with miR-4722-3p ASO, and this was reversed by knockdown of N13.3. In other words, the results revealed that downregulation of N13.3 suppressed CRC progression via sponging miR-4722-3p.

In general, lncRNAs act in part to affect the progression of cancers by targeting miRNA/protein axis (25). P2RY8 was found to form the P2RY8-CRLF2 fusion and participate in the hallmarks of B-progenitor acute lymphoblastic leukaemia (ALL) progression (27). However, the studies on P2RY8 were mainly carried out in ALL (28-30). In the present study, we predicted P2RY8 as a potential downstream target of miR-4722-3p for the first time, and confirmed the prediction using the luciferase reporter assay. Further results showed that P2RY8 was aberrantly upregulated in CRC cancer tissues and cell lines as compared to the control groups. In addition, the loss and gain experiments of miR-4722-3p indicated the negative regulation of miR-4722-3p by P2RY8 by RT-qPCR and western blot analysis. Simultaneously, we also found that N13.3 was positively correlated with P2RY8. Therefore, this result confirmed that N13.3 promoted the development and progression of CRC by the miR-4722-3p/P2RY8 axis.

In cancer tissues of CRC patients, we found that the expression of N13.3 and P2RY8 were significantly increased, while the expression of miR-4722-3p was decreased when compared with the normal tissues. Based on the fact that the cancer tissue used in this study was obtained from patient tissues during surgery, it is possible to determine the progression of CRC patients by detecting the changes in the expression of the above indices. For instance, the increased expression of N13.3 and P2RY8 may indicate the aggravation of the patient's condition. In addition, our results showed that the expression of N13.3 was closely related to the poor prognosis of the CRC patients. Moreover, the survival rate of CRC patients having high expression of N13.3 was significantly lower than that of the patients having low expression of N13.3. Therefore, it may be possible to predict the survival of CRC patients by detecting the expression level of N13.3. Although our study was the first to determine that there is a differential expression pattern of NA13.3, miR-4722-3p and P2RY8 in patients with CRC, there are few studies on NA13.3, miR-4722-3p and P2RY8 in patients with CRC. In this regard, further studies are needed to determine the specific role of NA13.3, miR-4722-3p and P2RY8 in CRC patients. Our follow-up study will further reveal the interaction between them.

In conclusion, our study, for the first time, identified the critical role of the N13.3/miR-4722-3p/P2RY8 axis in CRC progression, and this may provide a new insight for the clinical diagnosis and treatment of CRC.

Acknowledgements

Not applicable.

Funding

The present study was supported by the National Natural Science Foundation of China (81660410), the Yunnan Natural Science Foundation of China [2017FE468(-174), 2015HB073] and the Yunnan Science and Technology Project (2015HB073, L-2017018).

Availability of data and materials

The datasets used during the present study are available from the corresponding author upon reasonable request.

Authors' contributions

SB and HY conceived and designed the study. HY, QL, YW, JD, YL, ZD, CX and JF performed the experiments. SB and

HY wrote the manuscript. All authors analyzed data, revised the manuscript, and read and approved the final version of the manuscript.

Ethics approval and consent to participate

The protocol involving human participants was approved by the Ethics Committee of The First Affiliated Hospital of Kunming Medical University (Kunming, China) and written informed consent was obtained from all participants. The animal experimental protocol was approved by the Ethics Committee of The First Affiliated Hospital of Kunming Medical University.

Patient consent for publication

Not applicable.

Competing interests

The authors declare that they have no competing interests.

References

1. Arnold M, Sierra MS, Laversanne M, Soerjomataram I, Jemal A and Bray F: Global patterns and trends in colorectal cancer incidence and mortality. Gut 66: 683-691, 2017.
2. Xu L, Li X, Cai M, Chen J, Li X, Wu WK, Kang W, Tong J, To KF, Guan XY, *et al*: Increased expression of Solute carrier family 12 member 5 via gene amplification contributes to tumour progression and metastasis and associates with poor survival in colorectal cancer. Gut 65: 635-646, 2016.
3. Ozawa T, Matsuyama T, Toiyama Y, Takahashi N, Ishikawa T, Uetake H, Yamada Y, Kusunoki M, Calin G and Goel A: CCAT1 and CCAT2 long noncoding RNAs, located within the 8q.24.21 'gene desert', serve as important prognostic biomarkers in colorectal cancer. Ann Oncol 28: 1882-1888, 2017.
4. Stein A, Atanackovic D and Bokemeyer C: Current standards and new trends in the primary treatment of colorectal cancer. Eur J Cancer 47 (Suppl 3): S312-S314, 2011.
5. Song W, Tiruthani K, Wang Y, Shen L, Hu M, Dorosheva O, Qiu K, Kinghorn KA, Liu R and Huang L: Trapping of lipopolysaccharide to promote immunotherapy against colorectal cancer and attenuate liver metastasis. Adv Mater 30: e1805007, 2018.
6. Downing A, Morris EJ, Corrigan N, Sebag-Montefiore D, Finan PJ, Thomas JD, Chapman M, Hamilton R, Campbell H, Cameron D, *et al*: High hospital research participation and improved colorectal cancer survival outcomes: A population-based study. Gut 66: 89-96, 2017.
7. Azvolinsky A: Colorectal cancer: To stack or sequence therapy? J Natl Cancer Inst 107: djv138, 2015.
8. Shi X, Sun M, Liu H, Yao Y and Song Y: Long non-coding RNAs: A new frontier in the study of human diseases. Cancer Lett 339: 159-166, 2013.
9. Liu Q, Huang J, Zhou N, Zhang Z, Zhang A, Lu Z, Wu F and Mo YY: LncRNA loc285194 is a p53-regulated tumor suppressor. Nucleic Acids Res 41: 4976-4987, 2013.
10. Yao N, Fu Y, Chen L, Liu Z, He J, Zhu Y, Xia T and Wang S: Long non-coding RNA NONHSAT101069 promotes epirubicin resistance, migration, and invasion of breast cancer cells through NONHSAT101069/miR-129-5p/Twist1 axis. Oncogene 38: 7216-7233, 2019.
11. Zheng J, Zhang H, Ma R, Liu H and Gao P: Long non-coding RNA KRT19P3 suppresses proliferation and metastasis through COPS7A-mediated NF-κB pathway in gastric cancer. Oncogene 38: 7073-7088, 2019.
12. Yuan W, Sun Y, Liu L, Zhou B, Wang S and Gu D: Circulating lncRNAs serve as diagnostic markers for hepatocellular carcinoma. Cell Physiol Biochem 44: 125-132, 2017.
13. Arriaga-Canon C, De La Rosa-Velázquez IA, González-Barrios R, Montiel-Manríquez R, Oliva-Rico D, Jiménez-Trejo F, Cortés-González C and Herrera LA: The use of long non-coding RNAs as prognostic biomarkers and therapeutic targets in prostate cancer. Oncotarget 9: 20872-20890, 2018.
14. Wang P, Ning S, Zhang Y, Li R, Ye J, Zhao Z, Zhi H, Wang T, Guo Z and Li X: Identification of lncRNA-associated competing triplets reveals global patterns and prognostic markers for cancer. Nucleic Acids Res 43: 3478-3489, 2015.
15. Wang Y and Zhang J: Identification of differential expression lncRNAs in gastric cancer using transcriptome sequencing and bioinformatics analyses. Mol Med Rep 17: 8189-8195, 2018.
16. Yang Y, Zhao Y, Zhang W and Bai Y: Whole transcriptome sequencing identifies crucial genes associated with colon cancer and elucidation of their possible mechanisms of action. Onco Targets Ther 12: 2737-2747, 2019.
17. Ren W, Zhang J, Li W, Li Z, Hu S, Suo J and Ying X: A tumor-specific prognostic long non-coding RNA signature in gastric cancer. Med Sci Monit 22: 3647-3657, 2016.
18. Shi X, Tan H, Le X, Xian H, Li X, Huang K, Luo VY, Liu Y, Wu Z, Mo H, *et al*: An expression signature model to predict lung adenocarcinoma-specific survival. Cancer Manag Res 10: 3717-3732, 2018.
19. Bradford JR, Cox A, Bernard P and Camp NJ: Consensus analysis of whole transcriptome profiles from two breast cancer patient cohorts reveals long non-coding RNAs associated with intrinsic subtype and the tumour microenvironment. PLoS One 11: e0163238, 2016.
20. Livak KJ and Schmittgen TD: Analysis of relative gene expression data using real-time quantitative PCR and the 2(-Delta Delta C(T)) method. Methods 25: 402-408, 2001.
21. Lan Y, Xiao X, He Z, Luo Y, Wu C, Li L and Song X: Long noncoding RNA OCC-1 suppresses cell growth through destabilizing HuR protein in colorectal cancer. Nucleic Acids Res 46: 5809-5821, 2018.
22. Huang JZ, Chen M, Chen D, Gao XC, Zhu S, Huang H, Hu M, Zhu H and Yan GR: A peptide encoded by a putative lncRNA HOXB-AS3 suppresses colon cancer growth. Mol Cell 68: 171-184.e6, 2017.
23. Ma Y, Yang Y, Wang F, Moyer MP, Wei Q, Zhang P, Yang Z, Liu W, Zhang H, Chen N, *et al*: Long non-coding RNA CCAL regulates colorectal cancer progression by activating Wnt/β-catenin signalling pathway via suppression of activator protein 2α. Gut 65: 1494-1504, 2016.
24. Xiang JF, Yin QF, Chen T, Zhang Y, Zhang XO, Wu Z, Zhang S, Wang HB, Ge J, Lu X, *et al*: Human colorectal cancer-specific CCAT1-L lncRNA regulates long-range chromatin interactions at the MYC locus. Cell Res 24: 513-531, 2014.
25. Li C, Zheng H, Hou W, Bao H, Xiong J, Che W, Gu Y, Sun H and Liang P: Long non-coding RNA linc00645 promotes TGF-β-induced epithelial-mesenchymal transition by regulating miR-205-3p-ZEB1 axis in glioma. Cell Death Dis 10: 717, 2019.
26. Zheng YJ, Zhao JY, Liang TS, Wang P, Wang J, Yang DK and Liu ZS: Long noncoding RNA SMAD5-AS1 acts as a microRNA-106a-5p sponge to promote epithelial mesenchymal transition in nasopharyngeal carcinoma. FASEB J 33: 12915-12928, 2019.
27. Mullighan CG, Collins-Underwood JR, Phillips LA, Loudin MG, Liu W, Zhang J, Ma J, Coustan-Smith E, Harvey RC, Willman CL, *et al*: Rearrangement of CRLF2 in B-progenitor- and Down syndrome-associated acute lymphoblastic leukemia. Nat Genet 41: 1243-1246, 2009.
28. Potter N, Jones L, Blair H, Strehl S, Harrison CJ, Greaves M, Kearney L and Russell LJ: Single-cell analysis identifies CRLF2 rearrangements as both early and late events in Down syndrome and non-Down syndrome acute lymphoblastic leukaemia. Leukemia 33: 893-904, 2019.
29. Vesely C, Frech C, Eckert C, Cario G, Mecklenbräuker A, Zur Stadt U, Nebral K, Kraler F, Fischer S, Attarbaschi A, *et al*: Genomic and transcriptional landscape of P2RY8-CRLF2-positive childhood acute lymphoblastic leukemia. Leukemia 31: 1491-1501, 2017.
30. Morak M, Attarbaschi A, Fischer S, Nassimbeni C, Grausenburger R, Bastelberger S, Krentz S, Cario G, Kasper D, Schmitt K, *et al*: Small sizes and indolent evolutionary dynamics challenge the potential role of P2RY8-CRLF2-harboring clones as main relapse-driving force in childhood ALL. Blood 120: 5134-5142, 2012.